

Review

AlH₃ as High-Energy Fuels for Solid Propellants: Synthesis, Thermodynamics, Kinetics, and Stabilization

Youhai Liu ¹, Fusheng Yang ^{1,*}, Yang Zhang ², Zhen Wu ¹ and Zaoxiao Zhang ¹

¹ School of Chemical Engineering and Technology, Xi'an Jiaotong University, Xi'an 710049, China; 4121116019@stu.xjtu.edu.cn (Y.L.); wuz2015@mail.xjtu.edu.cn (Z.W.); zhangzx@mail.xjtu.edu.cn (Z.Z.)

² Science and Technology on Combustion and Explosion Laboratory, Xi'an Modern Chemistry Research Institute, Xi'an 710065, China; aerozy@163.com

* Correspondence: yang.fs@mail.xjtu.edu.cn

Abstract: Aluminum hydride (AlH₃) has attracted wide attention due to its high gravimetric and volumetric hydrogen capacity. AlH₃ can easily release hydrogen when heated at relatively low temperature. Such high hydrogen density and low dehydrogenation temperature make it one of the most promising high-energy fuels for solid propellants. In particular, AlH₃ as a component of solid propellants may greatly increase the specific impulse of rocket engines. However, AlH₃ exhibits low chemical and thermal stability in an ambient atmosphere. In this paper, the research progress about the synthesis, dehydrogenation thermodynamics, and kinetics, the stabilization of AlH₃ over the past decades are reviewed, with the aim of exploring more a economical synthesis and suitable stabilization methods for large-scale use in solid propellants. Finally, some suggestions regarding future research directions in this filed are proposed.

Keywords: AlH₃; solid propellants; decomposition; synthesis; stability; high energy material



Citation: Liu, Y.; Yang, F.; Zhang, Y.; Wu, Z.; Zhang, Z. AlH₃ as High-Energy Fuels for Solid Propellants: Synthesis, Thermodynamics, Kinetics, and Stabilization. *Compounds* **2024**, *4*, 230–251. <https://doi.org/10.3390/compounds4020012>

Academic Editors: Juan C. Mejuto and Takashiro Akitsu

Received: 30 December 2023

Revised: 25 February 2024

Accepted: 20 March 2024

Published: 26 March 2024



Copyright: © 2024 by the authors. Licensee MDPI, Basel, Switzerland. This article is an open access article distributed under the terms and conditions of the Creative Commons Attribution (CC BY) license (<https://creativecommons.org/licenses/by/4.0/>).

1. Introduction

Solid propellants act as the power source of the rocket motor and play an important role in the fields of military and aerospace. The pursuit of higher energy solid propellants has always been an inevitable requirement for the development of solid rockets. Metal hydrides possess high combustion heats due to the introduction of “hydrogen energy”, thus making them promising candidates for the solid fuels of propellants. In addition, considering that a decrease in the average molecular weight of gas combustion products will lead to an increase specific impulses of propellants, the low-molecular-weight H₂ produced by hydride decomposition makes them more attractive.

In recent years, considerable efforts have been made to evaluate the potential of hydrides as energy fuels for solid propellants, including aluminum hydride (AlH₃) [1–3], lithium hydride (LiH) [4], magnesium hydride (MgH₂) [5,6], titanium hydride (TiH₂) [7,8], and ammonia borane (NH₃BH₃) [9]. Table 1 summarizes the hydrogen storage properties of common metal hydrides. Among the above hydrides, AlH₃ is regarded as an important promising candidate due to its high heat of combustion (about 40 MJ/kg), volumetric hydrogen storage densities (148 kgH₂/km³) and hydrogen content (10.1 wt%). For example, when replacing 18% of aluminum (Al), a widely used metallic fuel in solid propellants, in a conventional ammonium perchlorate/hydroxyl-terminated polybutadiene (AP/HTPB)-based rocket propellant with aluminum hydride (AlH₃), the theoretical specific impulse would increase by 10%, and the flame temperature would decrease by 5%.

AlH₃ is a polyphasic substance, with no less than seven non-solvated crystal forms, namely α , α' , β , γ , δ , ϵ , and ζ -AlH₃, due to different synthesis routes and reaction conditions. It is generally believed that the α -AlH₃ phase is the dominant phase, while the other phases are usually considered as impurity products of the α -AlH₃ phase, and they are not as stable as α -AlH₃. Some of them directly decompose into elements, while the other ones

convert to α -AlH₃ before further decomposition. Therefore, α -AlH₃ deserves much more investigation [10,11]. However, α -AlH₃ is very sensitive to oxidants and could easily decompose into aluminum in an atmospheric environment [12]. Due to the poor stability of AlH₃, during long-term storage process, the slight decomposition of AlH₃ at room temperature promotes the generation and development of cracks in the solid propellant grain and reduces the propellant performance. In addition, the poor compatibility of α -AlH₃ with certain propellant components, such as nitrates, further limits its application in solid propellants [13].

Table 1. The hydrogen storage properties of common metal hydrides.

Hydrides	Molar Mass (g/mol)	Density (g/cm ³)	Gravimetric Hydrogen Density (wt%)	Volumetric Hydrogen Density (kg/m ³)	T _{dec} (K)
LiH	7.95	0.82	11.5	98.3	474.15
MgH ₂	26.31	1.45	7.6	110	674.15
TiH ₂	49.89	3.91	4.0	91.0	624.15
NH ₃ BH ₃	30.81	0.78	19.6	145	399.15
BeH ₂	11.03	0.65	18.28	71.2	524.15
AlH ₃	30.0	1.477	10.1	148	434.15

A large quantity of endeavors have been tried on the synthesis and stabilization of α -AlH₃ [14–20], aiming at producing products with better stability, higher quality, and more energy as additive fuel for solid propellants. This review focuses on the relevant research about the above-mentioned aspects; meanwhile, thermal decomposition properties and stabilization methods were also proposed. The paper is organized as follows. Firstly, Section 2 presents the synthesis methods of aluminum hydride. Next, the thermodynamics and kinetics of AlH₃ are described in Section 3. Thirdly, Section 4 summarizes the physical and chemical modification methods of AlH₃ to achieve the purpose of stabilizing aluminum hydride. Finally, we propose potential future research directions and aim to offer a valuable reference for subsequent studies on AlH₃ in related fields.

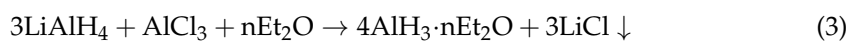
2. Synthesis of AlH₃

2.1. Wet Chemical Methods

Synthesis of AlH₃ has been studied since the 1940s, when Stecher and Wiberg first synthesized AlH₃·2N(CH₃)₃ in a low and impure form. Later, wet chemistry method was first reported by Finholt et al. [21], but the ether cannot be completely removed at that time, so the products were mainly solvated α -AlH₃.



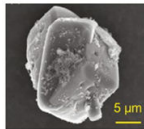
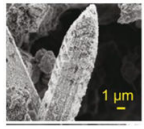
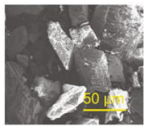
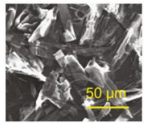
Brower et al. [22] synthesized seven non-solvated AlH₃ polymorphs, which are now commonly referenced when preparing AlH₃. The process consists of two steps. Firstly, LiAlH₄ (or LiH) and AlCl₃ react in ether solution to form AlH₃-ether complex and LiCl precipitate, seen in Reaction (1). Secondly, the ether ligand was removed through heating the product, which is also called post-crystallization, as shown in Reaction (2). Finally, the products need to undergo an ether solvent wash to eliminate any surplus LiAlH₄ or LiBH₄, followed by vacuum drying to produce the final AlH₃.



According to Refs. [23–26], the synthesis process of the AlH_3 polymorphs depends on multiple conditions, such as temperature, time, the presence of $\text{LiAlH}_4/\text{LiBH}_4$ or not, and the atmosphere. Generally, the $\gamma\text{-AlH}_3$ can be obtained from the desolvation reaction of etherate AlH_3 in the presence of only LiAlH_4 at lower temperature ($60\sim 70\text{ }^\circ\text{C}$), whereas the $\alpha\text{-AlH}_3$ can be obtained from the desolvation reaction of etherate AlH_3 in the presence of excess LiBH_4 and LiAlH_4 . Pure $\beta\text{-AlH}_3$ or $\alpha'\text{-AlH}_3$ are difficult to prepare and usually form accompanying with $\gamma\text{-AlH}_3$. However, no reproducible synthesis methods of the $\delta\text{-}$, $\epsilon\text{-}$, and $\zeta\text{-AlH}_3$ were established.

Table 2 displays the preparation conditions and properties of various AlH_3 polymorphs. Additionally, a more efficient method for synthesizing high-purity $\alpha\text{-AlH}_3$ crystals involves directly dissolving the reactants in ether and toluene, respectively.

Table 2. The preparation conditions and characteristics of different AlH_3 polymorphs.

Polymorphs	Experiment Conditions			Size of Product	Structure	Space Group	Morphology
	$\text{LiAlH}_4:\text{AlCl}_3:\text{LiBH}_4$	T ($^\circ\text{C}$)	Time				
$\alpha\text{-AlH}_3$	1:4:1	65	6.5 h	60 nm	a = 4.449 Å c = 11.804 Å	$R\bar{3}c$	
	1:3:0	85–93	2–8 h	6–13 μm			
	(PDMS, HCl)	62	11 h	50–100 μm			
	1:4:0 ($\gamma \rightarrow \alpha$) 1:4:1 ($\beta \rightarrow \alpha$)	65	6 h				
$\alpha'\text{-AlH}_3$	1:4:0	60	4 h	1 μm	a = 6.470 Å b = 11.117 Å c = 6.562 Å	$Cmcm$	
$\beta\text{-AlH}_3$	1:4:1	75	6 h	<50 μm	a = 9.004 Å	$Fd\bar{3}m$	
$\gamma\text{-AlH}_3$	1:4:0	65	45 min	<50 μm	a = 7.336 Å b = 5.367 Å c = 5.765 Å	$Pnmm$	

For wet synthesis methods, the formation of $\text{AlH}_3\cdot\text{Et}_2\text{O}$ requires a large amount of environmentally harmful organic solvents, like ethers or amines. Furthermore, the costly removal and recycling of these organic solvents, coupled with the challenge of controlling the preparation conditions due to the reaction's high sensitivity to temperature and time, make achieving the desired polymorph difficult [27]. Conditions control, solvent reuse, and other factors make it relatively difficult to scale up the synthesis of AlH_3 using wet methods.

2.2. Dry Synthesis Methods

As mentioned above, wet synthesis of AlH_3 requires a large amount of solvents, often being expensive and toxic. Therefore, numerous methods for the synthesis of AlH_3 without solvents, generally termed dry synthesis methods, have been proposed [28–34].

2.2.1. Mechano-Chemical Method

The mechano-chemical method is considered more environmentally friendly and cost-effective than traditional wet chemical methods, and has been used to prepare numerous aluminum hydrides, such as $\text{Mg}(\text{AlH}_4)_2$ [35,36], $\text{Ca}(\text{AlH}_4)_2$ [37,38], and $\text{LiMg}(\text{AlH}_4)_3$ [39]. Many studies have demonstrated that this solvent-free method has lower energy consumption than traditional wet synthesis process [30,31], and only necessitates inexpensive metal hydrides (such as LiH , NaH , CaH_2 , and MgH_2) instead of LiAlH_4 , making it an increasingly popular alternative method for AlH_3 preparation.

Duan et al. [29,40] investigated the synthesis of AlH_3 by reactive milling using aluminum chloride and cheap metal hydrides as starting materials. XRD and NMR analyses indicated that nano-sized materials AlH_3 were prepared using commercial AlCl_3 and nanocrystalline MgH_2 as reagents.

Duan et al. [30,41] also reported that $\alpha\text{-AlH}_3$ nanocomposites can be obtained by adding TiF_3 to LiH and AlCl_3 systems through ball milling in a short period of time, where suitable gas and pressure conditions can completely suppress the formation of metallic Al. The results indicate that TiF_3 plays a synergistic role in the solid-state reaction between LiH and AlCl_3 , and has significantly affect dehydriding properties of AlH_3 , compared to the $\alpha\text{-AlH}_3/\text{LiCl}$ nano-composite without TiF_3 . The as-milled $\alpha\text{-AlH}_3/\text{LiCl-TiF}_3$ composite has a hydrogen desorption of 9.92 wt% at 160 °C within 750 s, which is very close to the theoretical hydrogen capacity of AlH_3 .

However, this method is not suitable for large-scale commercial applications due to prohibitively high energy consumption. In addition, it's hard to get a pure product since slight decomposition of AlH_3 is almost inevitable during process.

2.2.2. Organoaluminum Decomposition Method

Organoaluminum decomposition is a method for directly preparing AlH_3 without the need for ether solvents [42]. The presence of surfactants enables the obtainment of AlH_3 through the decomposition of triethylaluminum under a hydrogen pressure of 10 MPa. The following illustrates the decomposition pathways of Et_3Al : $\text{Et}_3\text{Al} \rightarrow \text{Et}_2\text{AlH} \rightarrow \text{AlH}_3 \rightarrow \text{Al}$. In order to inhibit the further decomposition of generated AlH_3 into Al, the second step of decomposition reaction, i.e., $\text{Et}_2\text{AlH} \rightarrow \text{AlH}_3$, needs to be carried out at low temperature. In addition, Tetroctyl ammonium bromide (TOAB) and tetrabutylammonium bromide (TBAB) are used as surfactants to stabilize Al/ AlH_3 particles.

Figure 1 shows the TEM and EDS of as-prepared organo- AlH_3 (TOAB and TBAB as the surfactants). When TBAB is used as a surfactant, the particles obtained are relatively large, exceeding 100 nm in size and exhibit a regular spherical shape. In contrast, AlH_3 with an irregular morphology and with sizes ranging from 1 to 30 nm can be observed around the periphery of MgH_2 particles when TOAB is employed as the surfactant.

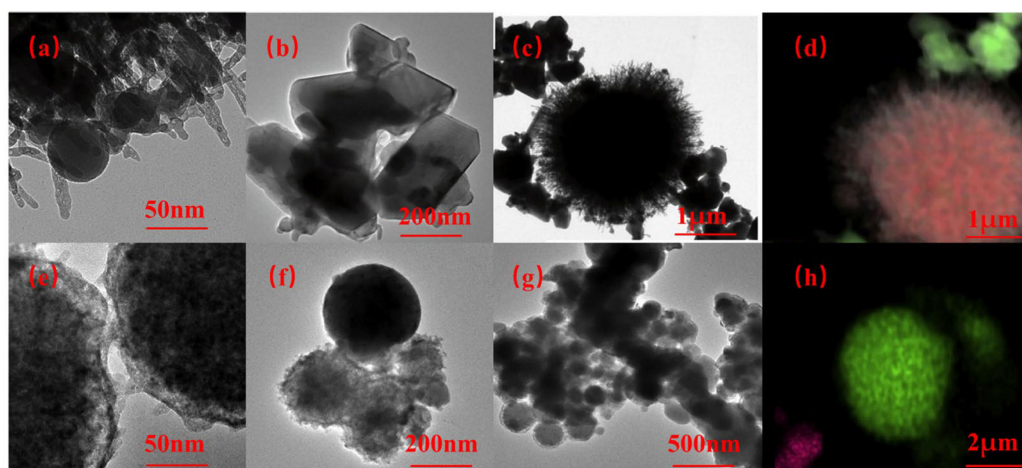


Figure 1. TEM and EDS images of AlH_3 with TOTB (a–d) and TBAB (e–h) synthesized via Et_3Al thermal decomposition. Reproduced with permission from Ref. [42]. Copyright 2018, Elsevier.

It is challenging to utilize organoaluminum decomposition to achieve high-purity AlH_3 products because of the presence of surfactants. Particularly, when TBAB is used as a surfactant, the synthesized particles exhibit poor stability and low decomposition temperature, limiting its application to propellants.

2.3. Other Emerging Methods

2.3.1. Supercritical Synthesis Method

Supercritical synthesis involves the dissolution and reaction of raw materials in supercritical media. Take AlH_3 as an example: it can be prepared by reacting activated aluminum with hydrogen in a supercritical liquid at $60\text{ }^\circ\text{C}$ for 1 h. [43,44]. The supercritical medium consists of supercritical liquid CO_2 in combination with an ether co-solvent. However, due to the use of liquid CO_2 , the reaction temperature cannot be further increased, and hence limits the reaction activity. The synthetic method is currently in the laboratory stage and still has a long way to go before achieving industrial-scale production.

2.3.2. Organoaluminum Decomposition Method

In the electrolyte solution, active aluminum powder and ionic state hydrogen encounter to trigger an electrochemical reaction, generating AlH_3 in the form of precipitation at the bottom of the electrolyte solution.

Zidanet et al. [45] used the Al as the anode and Pt as cathode, respectively, and the whole electrochemical process was realized in the NaAlH_4 -THF electrolyte. As shown in the reaction paths (Reactions (5) and (6)), AlH_3 can be produced via two distinct reaction mechanisms at the Al electrode, involving the oxidation of ions and the reaction of AlH_4^- with the Al anode. Based on this, a cycle using electrolysis and catalytic hydrogenation to treat waste aluminum was proposed [46] (see in Figure 2), in which the problem of the high hydrogen pressure and the formation of stable by-products such as LiCl could be avoided. It is noteworthy that the addition of LiCl is notable for its ability to enhance the yield of AlH_3 ; meanwhile, alkali hydride (e.g., LiH , NaH and KH) could be reformed through electrochemical potential.

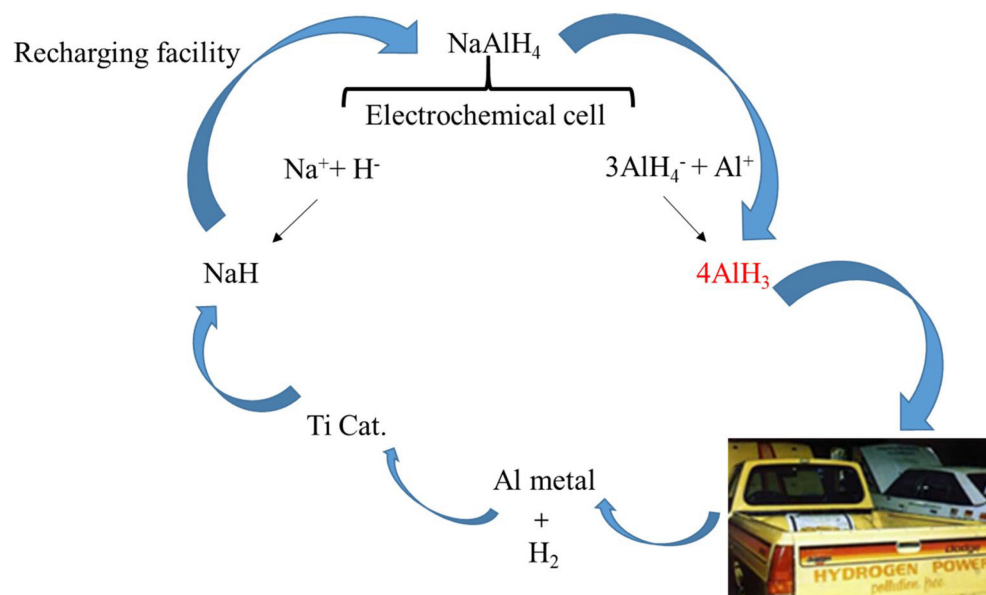
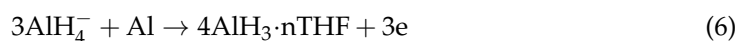
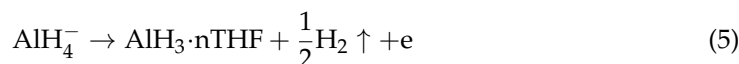


Figure 2. Proposed reversible fuel cycle for AlH_3 .

2.3.3. High Pressure Hydrogenation Method

The absorption of hydrogen by aluminum occurs under high pressure without modification, and could be utilized to prepare AlH_3 . However, the process necessitates a hydrogen pressure exceeding 700 MPa at ambient temperature. Saitoh et al. [47] studied

the reaction process of aluminum and hydrogen at 10 GPa and 600 °C using in situ X-ray diffraction. As shown in Figure 3, The yellow and red particles represent Al and AlH₃ particles, respectively. After 24 h growth, the grain size of AlH₃ was about 20 μm. The author also found that the growth process of an AlH₃ single crystal will go through three stages: self-pulverization of aluminum (with the increase of reaction time, it is found that the size of aluminum Bragg lattice decreases), hydrogenation of pulverized aluminum (X-ray diffraction image shows a new Bragg lattice), and solid-state grain growth of AlH₃.

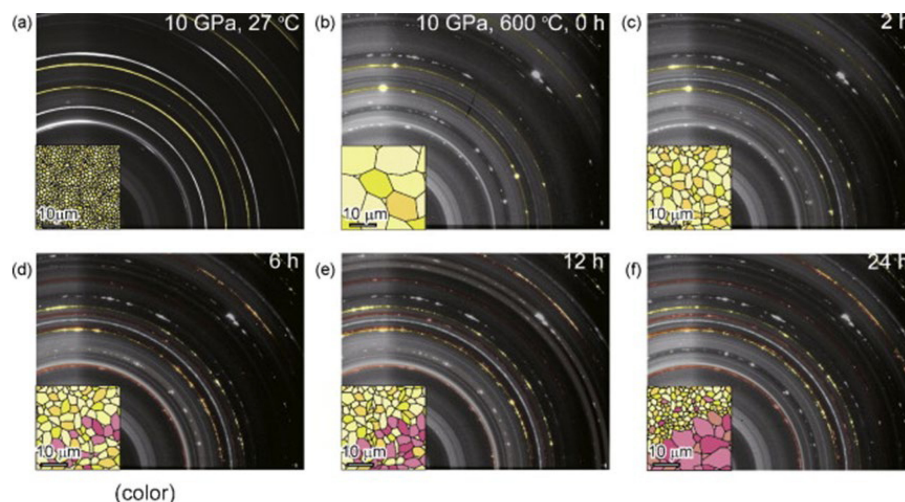


Figure 3. X-ray diffraction patterns and crystal growth process of Al/AlH₃ during high-pressure hydrogenation. (a) Complete Debye rings from aluminum at 10 GPa, 27 °C; (b) Bragg spots from aggregated aluminum (colored in yellow). This image was captured immediately after the sample was heated to 600 °C at 10 GPa; (c–f) Diffraction images taken after 2 h, 6 h, 12 h, and 24 h of heat treatment at 10 GPa and 600 °C. Reprinted with permission from Ref. [47]. Copyright 2010, Elsevier.

The formation of AlH₃ through Al hydrogenation is elucidated, wherein AlH₃ particles grow into a single crystal through solid-state grain growth. In addition, even at elevated pressures and temperatures, the hydrogenation reaction can be restricted by the chemically stable oxide layer on the surface of Al. The thickness of the surface oxide layer is crucial in altering the growth of single crystals. Given the demanding reaction conditions and low yield, the direct reaction of aluminum and hydrogen under high pressure to produce AlH₃ is not deemed a viable option.

2.4. Comparison of Synthetic Methods and Its Development Suggestion

To summarize, each method has its own advantages and disadvantages. Table 3 summarizes the common synthesis methods of aluminum hydride and some suggestions for development.

Table 3. Comparison of AlH₃ synthetic methods and its development proposal.

Methods	Advantages	Disadvantages	Development Suggestion
Wet chemical methods	1. High product quality and yield. 2. Simple process.	1. Large amount of organic solvents used. 2. Flammable raw materials, intermediates and solvents.	Improving the safety control level and synthesis process.
Dry synthesis methods	No or small amount of solvent used.	1. Serious aggregation of AlH ₃ crystals. 2. Difficult to separate AlH ₃ from by-products.	Developing suitable reaction conditions, synthesis devices, and purification technology.

Table 3. Cont.

Methods	Advantages	Disadvantages	Development Suggestion
Supercritical synthesis method	Direct reaction of activated Al with H ₂ .	The reaction activity is limited by the relatively low temperature	Break the limits of the reaction temperature by suitable medium.
Organoaluminum decomposition method	Cheap raw materials.	1. Low yield. 2. De-etherification and crystal transformation process of intermediate involved.	Developing low-cost exploratory research.
High pressure hydrogenation method	Direct reaction of Al with H ₂ .	1. Harsh reaction conditions. 2. Impurities. 3. Low yield.	Developing mild reaction conditions.

3. Thermodynamics and Kinetics of AlH₃

3.1. Thermodynamics

Aluminum hydride is known to degrade over time (after three days). This degradation can impact the stability and effectiveness of AlH₃ as a hydrogen storage material. α -AlH₃ can decompose directly into Al and H₂ through a single endothermic step (7). Sinke et al. [48] first investigated the thermodynamic properties of α -AlH₃, and the formation enthalpy was measured to be $-11.4 \text{ kJ mol}^{-1}$ at 25 °C. The less stable polymorphs α' , β , and γ -AlH₃ will undergo an exothermic transition to α -AlH₃ (8) at around 100 °C [49–51], whereas δ , ϵ , and ζ -AlH₃ would direct decomposition into Al without undergoing any crystal transformation. However, the direct decomposition of α' -AlH₃ and γ -AlH₃ into Al and H₂ was also observed (9) [50,52–54]. Liu et al. [53] studied the decomposition mechanisms of γ -AlH₃ and suggested that the outer layer of the γ -AlH₃ particle is more likely to undergo direct decomposition, while the inner part tends to become the more stable α -AlH₃ before decomposition (Figure 4). The enthalpies of the transition from α' , β , and γ -AlH₃ to α -AlH₃ were measured to be 1.6, 1.5, and 2.8 kJ/mol, respectively [50,55]. The formation enthalpy of approximately -10 kJ/mol was estimated for α -AlH₃ [55], and the value ranges from -9.5 to -9.9 kJ/mol for β or γ -AlH₃, while a low formation enthalpy of -2.5 kJ/mol was reported for α' -AlH₃ [50].

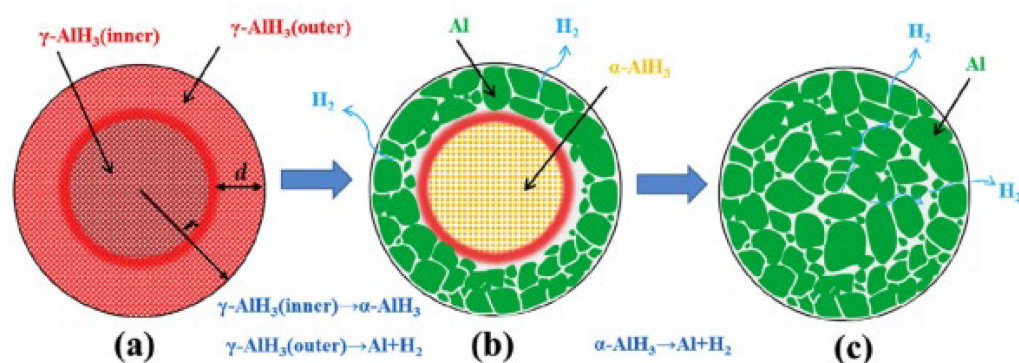
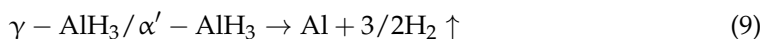
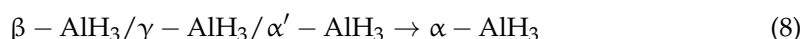


Figure 4. The dehydrogenation mechanism of γ -AlH₃. (a) as-synthesized γ -AlH₃; (b) after partial decomposition; (c) after full decomposition. reproduced with permission [53]. Copyright 2017, Elsevier.

Bulk AlH₃ is thermodynamically unstable (metastable) and is only kinetically stable under ambient conditions. Nanoscaling is a well-known strategy for destabilizing bulk metal hydrides, yielding faster rates of H₂ desorption, reduced formation of parasitic

intermediates, and greater reversibility. Stavila et al. [56] developed a new strategy for thermodynamic stabilization of metal hydrides by incorporating alane clusters within the pores of covalent triazine frameworks (CTF). The highly unfavorable thermodynamics of direct aluminum hydrogenation can be overcome by stabilizing alane within a nanoporous bipyridine-functionalized covalent triazine framework ($\text{AlH}_3\text{@CTF-bipyridine}$). The material desorb hydrogen at temperatures as low as 95 °C, with ca. 2/3 of the total hydrogen released within less than 10 min from the onset of dehydrogenation and can be partially rehydrogenated at 70 MPa (700 bar) H_2 (Figure 5). The results demonstrate that the strategy of thermodynamic stabilization through concomitant nanoconfinement could enable reversibility in high-capacity metastable metal hydrides.

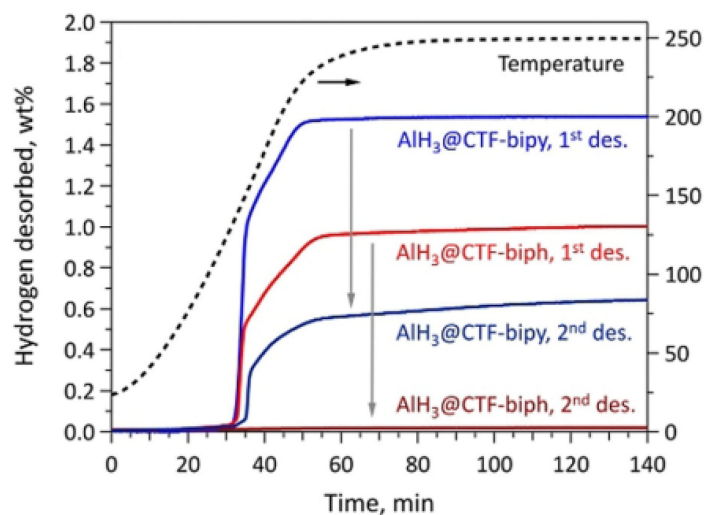


Figure 5. Sieverts data for $\text{AlH}_3\text{@CTF-biph}$ and $\text{AlH}_3\text{@CTF-bipy}$ samples prior and after the 700 bar (70 MPa) H_2 absorption cycle. Reproduced with permission [56] Copyright 2021, Wiley Online Library.

3.2. Kinetics

Herley et al. [57–59] firstly measured the thermal decomposition behavior of AlH_3 provided by DOW Chemical Company. The isothermal decomposition and TG-DSC curves of AlH_3 are shown in Figures 6a and 6b, respectively. The decomposition process is characterized by an endothermic step, and the isothermal decomposition curves of AlH_3 are usually divided into three parts: induction period, acceleratory period, and decay period. The induction period corresponds to the beginning of decomposition, and could be attributed to the crack of the surface layer. The acceleratory period results from rapid hydrogen release due to the multi-dimensional growth of aluminum [27]. The decay period marks the completion of the decomposition process. [23,27]. Therefore, through managing the time of induction period, the decomposition rate can be controlled [60]. In essence, controlling the formation of Al nuclei is the crucial factor in altering the decomposition rate.

The thermal reaction of AlH_3 in an air atmosphere is complex and can be categorized into three stages: dehydrogenation and passivation, primary oxidation, and secondary oxidation. It is noteworthy that the passivation process involving $\text{Al} \rightarrow \text{Al}_2\text{O}_3$, occurs almost simultaneously with the dehydrogenation reactions. An amorphous Al_2O_3 layer formed on the particles' surface by passivation encapsulates the contained hydrogen, and leads to incomplete dehydrogenation.

Milekhin et al. [61] employed TG-DSC, SEM, and EDS to study the dehydrogenation and oxidation kinetics and mechanisms of micron-sized $\alpha\text{-AlH}_3$ under various atmospheres, including nitrogen, argon, and air. The results indicated that the samples were stable below 150 °C, but can be decomposed between 150 and 180 °C. Figure 6 illustrates the theoretical kinetic model of AlH_3 in an oxidative environment.

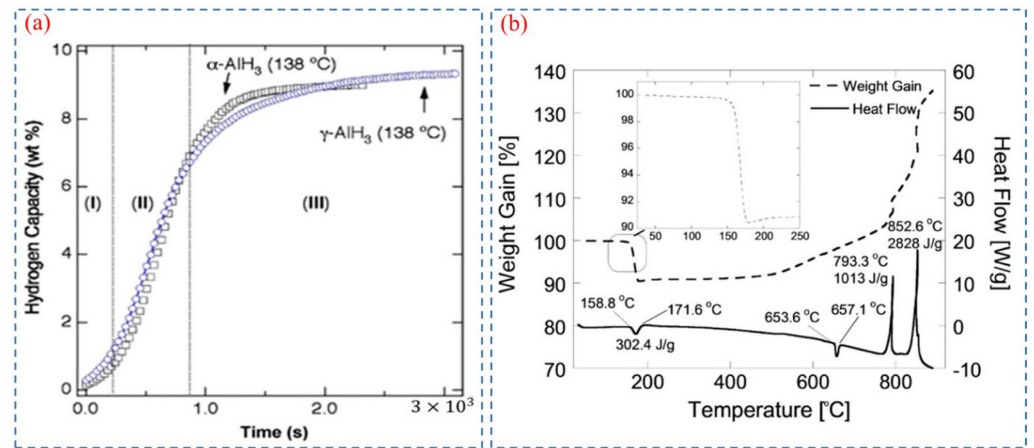


Figure 6. (a) Isothermal decomposition curves of α -AlH₃ and γ -AlH₃ [51]. Copyright 2007, Elsevier. (b) TGA and DSC of neat AlH₃ in an argon atmosphere [1]. Copyright 2019, Wiley Online Library.

Figure 7a depicts a schematic diagram illustrating the hydrogen decomposition on the surface of Aluminum hydride [62]. The process includes breakage of the surface oxide layer (e.g., Al₂O₃), recombination of hydrogen, and growth of aluminum [11]. The oxide layer surrounding AlH₃ particles is prone to cracking at elevated temperatures, as the volumetric thermal expansion of AlH₃ is approximately double that of amorphous and crystalline Al₂O₃. The results also indicate that hydrogen desorption begins only when the surface oxide layer breaks and the free AlH₃ on the surface of particles contact with the gas phase.

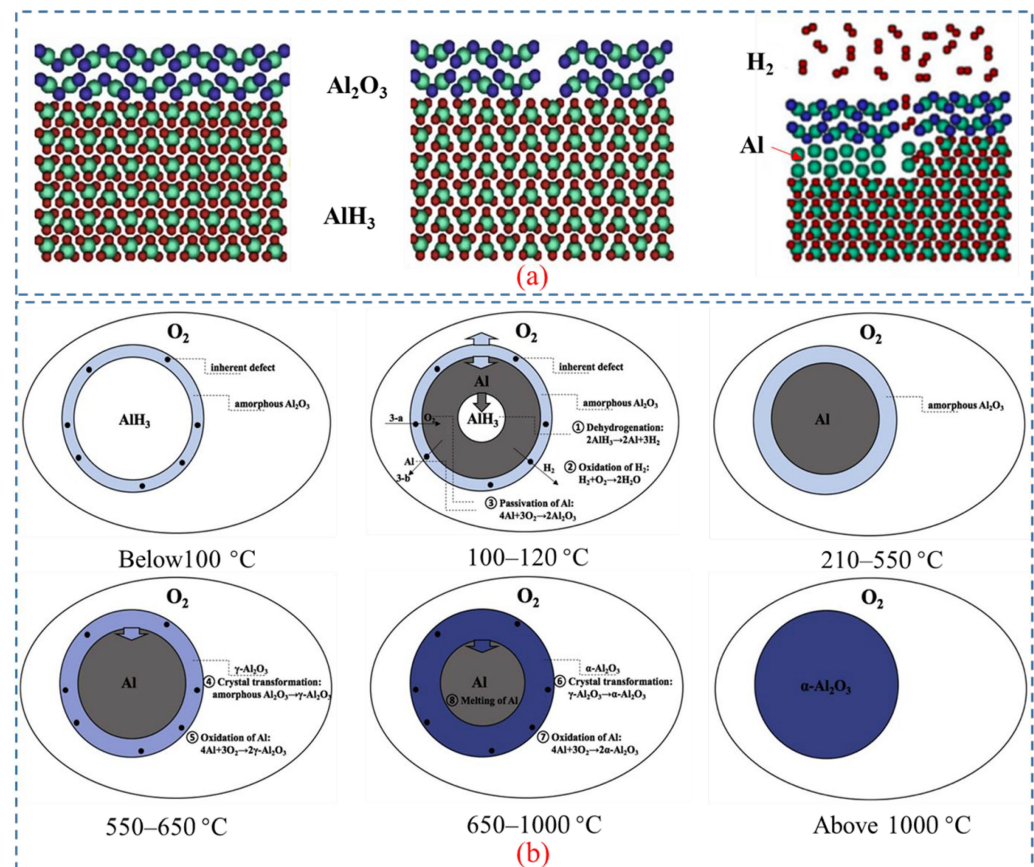


Figure 7. (a) The mechanism underlying hydrogen release from AlH₃ [62]. Copyright 2010, AIP Publishing. (b) The mechanism of dehydrogenation and oxidation of AlH₃ at different temperatures [10]. Copyright 2020, Elsevier.

Liu et al. [63] investigated the thermal oxidation of AlH_3 and proposed dehydrogenation/passivation mechanism. AlH_3 usually has a protective layer of Al_2O_3 on its surface, which inhibits the dehydrogenation reaction of AlH_3 at room temperature [44]. With the increase of temperature, cracks are formed in the Al_2O_3 layer, exposing the AlH_3 surface and causing the occurrence of incomplete dehydrogenation. Since the distance between Al atoms in AlH_3 is shorter than that in elemental Al, significant volume shrinkage will occur during the conversion of AlH_3 to Al [11,64], resulting in the formation of pores on the particle surface and further increase the exposed AlH_3 .

The transformation process of Al-containing substances during dehydrogenation and oxidation at different temperatures is shown in Figure 7b. The transition follows the route: $\alpha\text{-AlH}_3 \rightarrow \text{Al} \rightarrow \gamma\text{-Al}_2\text{O}_3 \rightarrow \alpha\text{-Al}_2\text{O}_3$. The reaction consists of decomposing of AlH_3 , oxidizing of H_2 , passivating of Al, and the crystal transition of Al_2O_3 to $\gamma\text{-Al}_2\text{O}_3$ and $\gamma\text{-Al}_2\text{O}_3$ to $\alpha\text{-Al}_2\text{O}_3$.

Dehydrogenation and oxidation of AlH_3 are influenced by three factors: the oxide layer, the surrounding atmosphere, and temperature. As mentioned above, decomposition only takes place when the oxide layer fractures, allowing free AlH_3 to come into contact with the surrounding atmosphere. Nakagawa et al. [65] investigated the effect of the thickness of the oxide layer on the dehydrogenation kinetics of $\alpha\text{-AlH}_3$. The TEM results (Figure 8) indicated that the thickness of Al_2O_3 seems to increase with exposure time through diffusion-controlled growth. Moreover, the peak temperatures during hand milling (135 °C) are significantly lower than those without milling (150 °C) under an argon atmosphere. This is believed to be due to the Al_2O_3 layer on the surface of AlH_3 , which may delay the dehydrogenation process. The Al_2O_3 and $\text{Al}(\text{OH})_3$ layer can also affect the dehydrogenation of AlH_3 . Yu et al. [66] prepared a novel core-shell structured $\alpha\text{-AlH}_3@ \text{Al}_2\text{O}_3@ \text{Al}(\text{OH})_3$ through hydrochloric acid leaching, which does not decompose under environmental conditions for several days. These findings suggest that the presence of an oxide layer can postpone the dehydrogenation process.

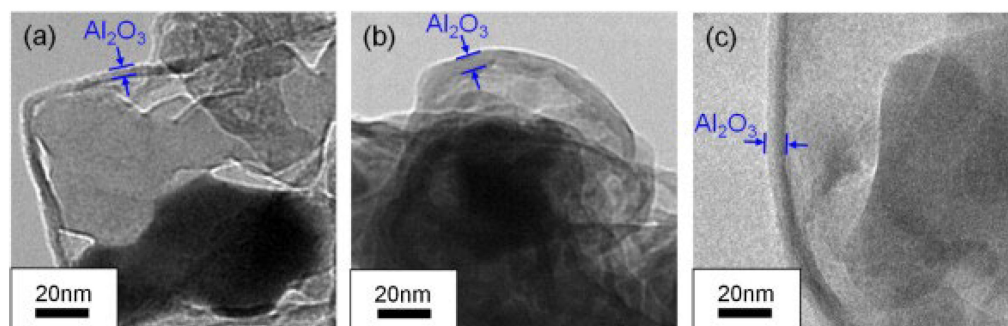


Figure 8. The TEM images of Al_2O_3 films on AlH_3 particles (a) without exposure to air, (b) one day after exposure to air, (c) seven days after exposure to air [65]. Copyright 2013, Elsevier.

The thermal reaction of AlH_3 is significantly influenced by the surrounding atmosphere, because different products could be generated with various gaseous, such as Al_2O_3 and AlN . Additionally, the dehydrogenation of AlH_3 is competitive with Al oxidation in an oxidative atmosphere. As illustrated in Figure 9, the surface agglomeration and roughness of particles in oxidative atmosphere are more obvious under elevating temperature.

The dehydrogenation and oxidation properties of AlH_3 are also affected by the heating rate and temperature. The impact of the heating rate was examined using a non-isothermal method. The results indicated that both the initial and final temperatures, as well as the final mass loss of the hydrothermal solution, decreased as the heating rate decreased. This reason can be attributed to the slower hydrogen diffusion through particles or nucleation at aluminum sites at lower temperatures and heating rates, resulting in some hydrogen remaining trapped in the particles [23].

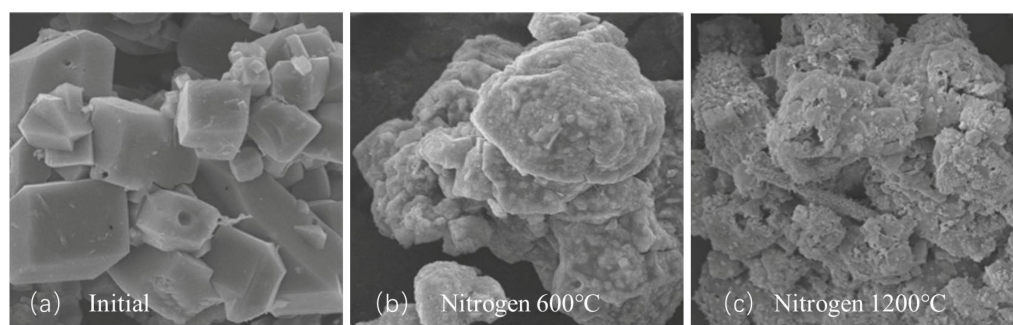


Figure 9. Microphotographs of the AlH_3 samples: (a) initial sample (b,c) after heating to 600 °C and 1200 °C in nitrogen medium, respectively. Reproduced with permission [61]. Copyright 2015, Springer.

4. Physical and Chemical Modification of AlH_3

Due to the low thermal stability of AlH_3 in ambient atmosphere, dehydrogenation will occur easily. The factors contributing to the instability of AlH_3 can be categorized into intrinsic and extrinsic causes. Regarding intrinsic causes, AlH_3 consists of two highly reducing elements, aluminum and hydrogen, with a small enthalpy of formation and positive Gibbs free energy [26,67,68]. Therefore, AlH_3 is in metastable state, and has a spontaneous tendency to decompose into aluminum and hydrogen from thermodynamic perspective.

On the other hand, impurities like LiCl , NaBH_4 , LiBH_4 , and LiAlH_4 , as well as unstable polymorphs formed during AlH_3 synthesis can also reduce its thermal stability [69]. Apart from this, other extrinsic factors, e.g., humidity, light, oxygen also make AlH_3 unstable.

When AlH_3 is used as a high-energy additive in propellants, to ensure its stable storage without decomposition and reduce the potential hazards during storage, transportation and use, it is necessary to stabilize AlH_3 , for which multiple methods are available, including surface passivation, doping, surface coating.

4.1. Surface Passivation Methods

In this method, some solutions, e.g., aqueous organic solution, buffer solution, and various acid solutions able to react with $\alpha\text{-AlH}_3$, are generally used. For one thing, the solutions can remove the synthetic impurities and unstable crystal forms. For another, they can shield against external stimuli by developing passivation layers of Al_2O_3 or $\text{Al}(\text{OH})_3$ on the surface of $\alpha\text{-AlH}_3$.

Nile et al. [70] treated $\alpha\text{-AlH}_3$ with n-butylamine containing a small amount of water. It took 60 days for the decomposition rate to reach 1%, while the untreated $\alpha\text{-AlH}_3$ reached the same decomposition rate in 13.5 days, indicating the stabilization effect of the treatment.

Robert et al. [71] used neutral buffer solution KH_2PO_4 and NaOH to treat $\alpha\text{-AlH}_3$ at 70 °C. The contents of impurities, e.g., C, Cl, and Li, in the particles were significantly reduced after 15 min, and the decomposition rate of $\alpha\text{-AlH}_3$ was also decreased, it took 26 days for the decomposition rate to reach 1% compared with 8 days without treated.

The $\alpha\text{-AlH}_3$ particles can also be stabilized using acid solutions. Typically, the acid choices include hydrochloric acid, hydrogen fluoride acid, hydrogen bromide acid, and others, with hydrochloric acid being the most preferable. Petrie et al. [17] used hydrochloric acid solution to clean $\alpha\text{-AlH}_3$. Meanwhile, the pickling process can also form Al_2O_3 or $\text{Al}(\text{OH})_3$ layer on the surface of the $\alpha\text{-AlH}_3$, which plays a stabilizing role. It took 12.7 days for $\alpha\text{-AlH}_3$ treated with hydrochloric acid solution to reach 1% decomposition at 60 °C, while the untreated $\alpha\text{-AlH}_3$ only takes 9.3 days. Figure 10 shows the SEM images of $\alpha\text{-AlH}_3$ before and after hydrochloric acid treatment. The results demonstrate that acid etching can eliminate cracks and impurities, expected to be beneficial to thermal stability of AlH_3 products [24].

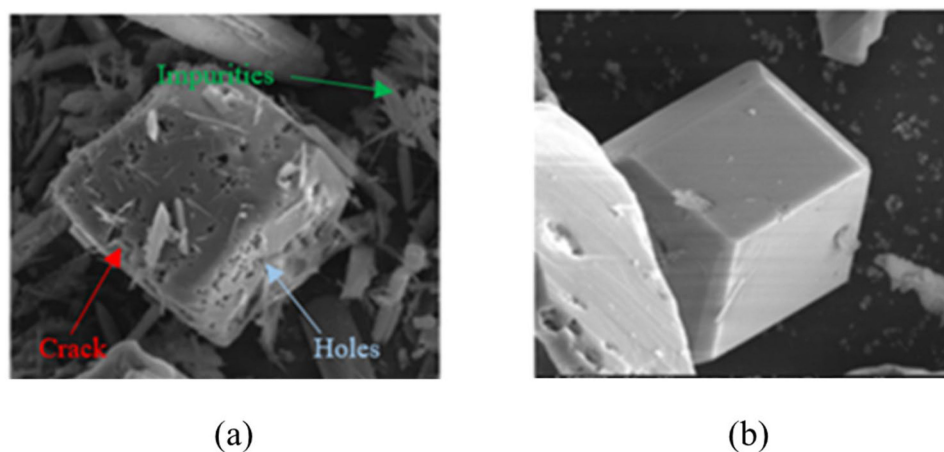


Figure 10. SEM images of α -AlH₃ (a) before and (b) after hydrochloric acid treatment.

The mechanism of hydrochloric acid stabilization of α -AlH₃ was investigated by Yu et al. [66]. They found that hydrochloric acid plays an important role in accelerating the hydrolysis reaction of AlH₃ to generate honeycomb-like structures which can generate integrity and dense oxide layers. Moreover, the detailed acid stabilization mechanism could be divided into surface oxidation, oxide layer rupture, hydrolysis reaction, and transition of oxide layers, as depicted in Figure 11.

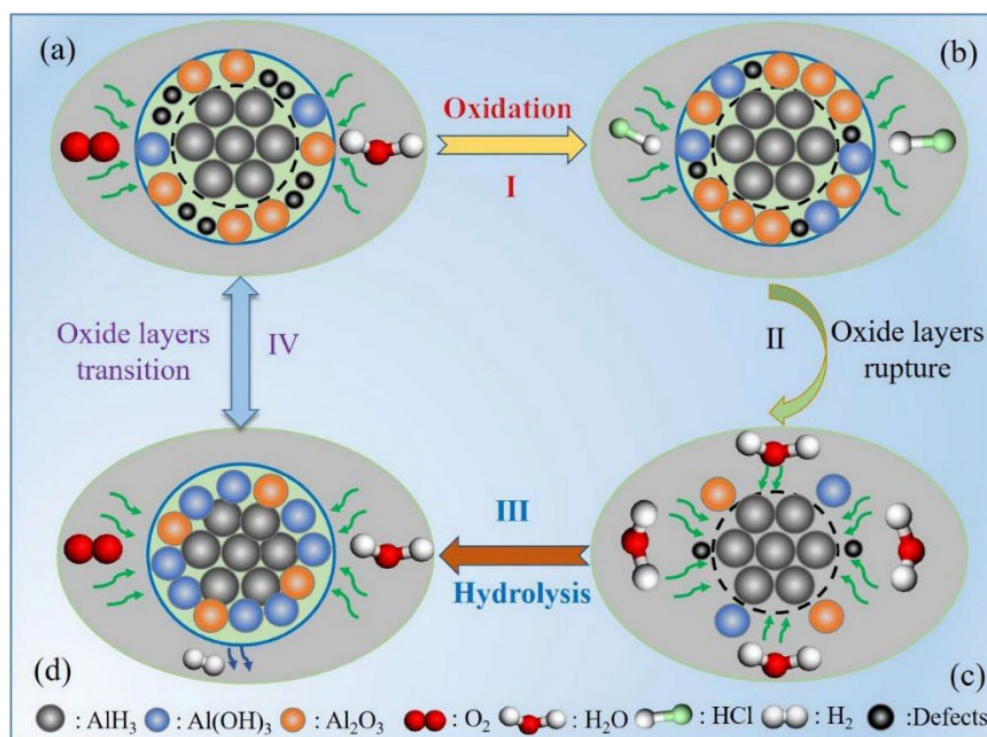


Figure 11. The stabilization mechanisms by acid passivation for AlH₃ [66]. (a) original structure; (b) surface oxidation; (c) oxide layers rupture and (d) honeycomb-like structure. Copyright 2022, Elsevier.

Additionally, surface passivation of AlH₃ can be achieved by heating it in air or an oxidizing atmosphere [72]. Despite the benefits to improve the thermal stability, the presence of an oxide layer by various passivation methods will inevitably cause the energy loss of α -AlH₃ and affect the combustion performance.

4.2. Doping Methods

The thermal stability of AlH_3 can be improved by doping following two approaches. One approach aims to eliminate the highly active sites in $\alpha\text{-AlH}_3$ crystal structure, hence increasing the activation energy of decomposition reaction. Norman et al. [73] added magnesium powder to the reaction of preparing $\alpha\text{-AlH}_3$, and the X-ray diffraction results showed varying degrees of expansion for the crystal structure of $\alpha\text{-AlH}_3$. It took 26 days for $\alpha\text{-AlH}_3$ doped with 2% magnesium powder to reach 1% decomposition rate in an anhydrous nitrogen atmosphere at 60 °C, while the undoped one only took 5 days. Cianciolo et al. [74] prepared $\alpha\text{-AlH}_3$ particles by doping $\alpha\text{-AlH}_3$ ether complexes with Hg. The experimental results indicated that the decomposition rate of $\alpha\text{-AlH}_3$ particles doped with 0.02% Hg is 0.4% at 100 °C for 24 h, far lower than the value of 9.4% of undoped particles under the same conditions. Furthermore, doping with other metal elements, such as Si, can also enhance the thermal stability of AlH_3 [74].

In theory, the decomposition of AlH_3 generates an electron hole caused by the formation of positively charged ions, while the Al^{3+} ions can further catalyze the surface decomposition of the bulk sample [75]. Therefore, the other approach is inhibiting the decomposition process by increasing the Lewis acid, Lewis base, or other compounds that can coordinate with Al^{3+} ions. It has been reported that the addition of such free radical inhibitors can enhance the thermal stability of AlH_3 by a factor of 10 to 20 [2]. For example, Alan et al. [76] doped AlH_3 using phenothiazine (PTA) or Mercaptobenzothiazole (MBT, as shown in Figure 12), making its decomposition rate only 0.97% after 27 days of storage at a constant temperature of 60 °C, far lower than that of untreated samples. Roberts et al. [77] doped aryl or alkyl-substituted silanols in the preparation process of $\alpha\text{-AlH}_3$. From their results, 8 and 4 days were reported for the decomposition rate to reach 1% for the doped and undoped $\alpha\text{-AlH}_3$, respectively.

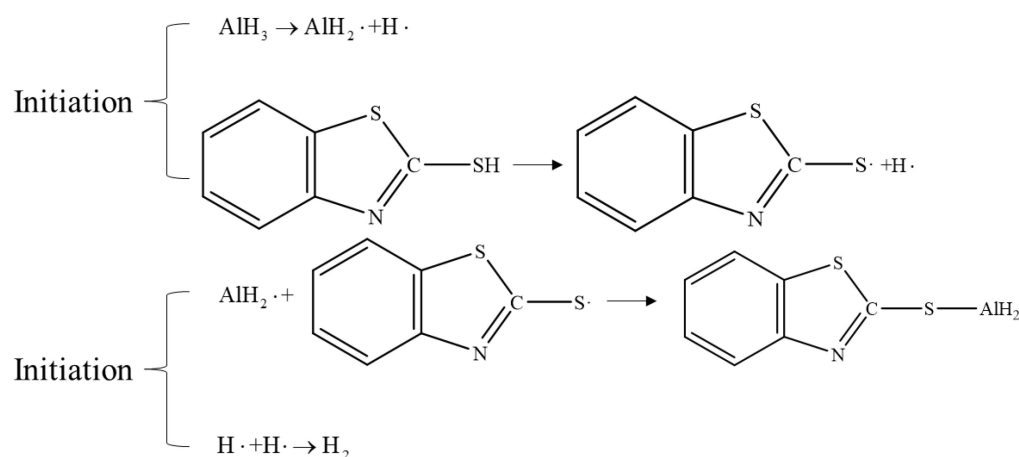


Figure 12. Stabilization mechanism of Mercaptobenzothiazole (MBT).

Similar to surface passivation methods, doping of $\alpha\text{-AlH}_3$ also results in a loss of energy due to decrease in the crystal purity of $\alpha\text{-AlH}_3$.

4.3. Surface Coating Methods

The surface coating method has received wide attention in recent years because it does not destroy the chemical reactivity of $\alpha\text{-AlH}_3$ [70,77]. Typically, the surface of AlH_3 is coated with inert and hydrophobic materials to create a core-shell structure, thereby altering its surface properties [78]. The structure not only prevents direct contact between the inner AlH_3 and humidity or oxygen but also reduces the number of active sites on the surface, thereby increasing the activation energy of the decomposition reaction [79]. Currently, coating materials mainly consist of inorganic and organic molecules, metal oxides, organic polymers, carbon materials, and some energetic components.

4.3.1. Inorganic and Organic Molecules

Norman et al. [80] used small gaseous (such as N_2F_4 , NO) and liquid molecules (such as Al_2S_3 , $AlCl_3$) to form a coating layer on the surface of $\alpha-AlH_3$ through an adsorption process. As a typical example, under $100\text{ }^\circ\text{C}$, the decomposition amount of the coated sample with NO molecule is reduced from 5.63% to 0.21%, for a duration of 7 h. In addition, after treatment with these small molecule stabilizers, $\alpha-AlH_3$ shows good compatibility with other propellant components, such as ammonium perchlorate and nitrocellulose.

Schmidt et al. [18] used organic compounds containing nitrile groups to coat $\alpha-AlH_3$, and the stability of AlH_3 was found to be enhanced through the bond interaction of nitrile groups and free radicals on its surface. Besides, the compatibility between $\alpha-AlH_3$ and propellant components was also improved.

Qin et al. [14] coated $\alpha-AlH_3$ with stearic acid, and no ignition was observed for the coated sample even when the value of electrostatic sensitivity (E_{50}) reached the test limit of 5390 mJ. In comparison, the E_{50} of $\alpha-AlH_3$ without coating is only 367 mJ.

Shi et al. [81] used a silane coupling agent, A171, to modify the surface of $\alpha-AlH_3$. The surface was uniformly covered with a thin organic layer via the coating process shown in Figure 13. After coating, the standard $100\text{ }^\circ\text{C}$ thermostatic thermal stability and activation energy of $\alpha-AlH_3$ increased up to 95.25 min and 4.32 kJ mol^{-1} , respectively.

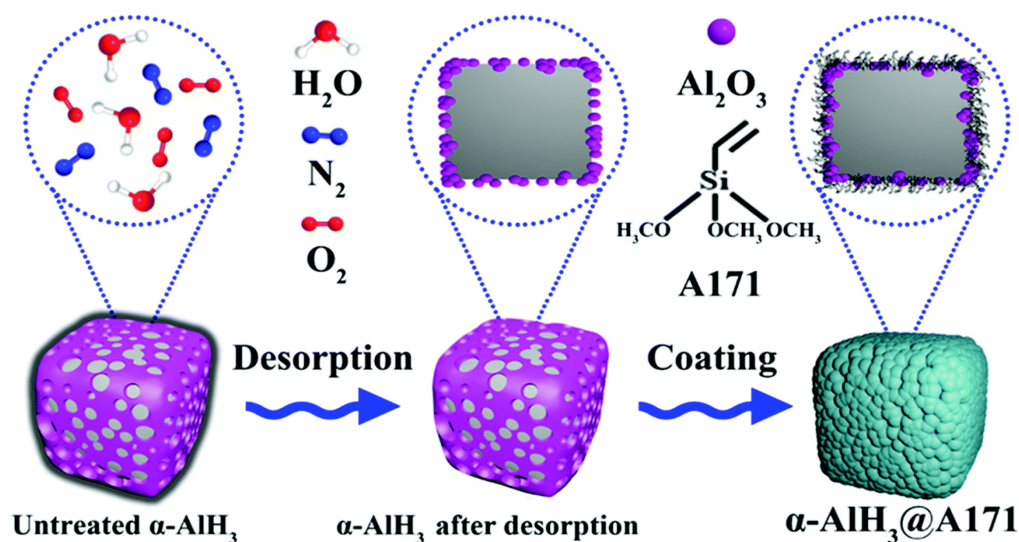


Figure 13. The preparation process of the $\alpha-AlH_3@A171$ composite [81]. Copyright 2022, Royal Society Chemistry.

4.3.2. Metal Oxides

Kempa et al. [82] found that the surface aluminum oxide layer of $\alpha-AlH_3$ can effectively isolate water and oxygen molecules in the environment so that the crystal structure of $\alpha-AlH_3$ does not change significantly for a long time. In recent years, researchers have tried to control the coating structure by atomic layer deposition (ALD) and other advanced techniques to achieve accurate control of the thermal stability of AlH_3 [83].

Chen et al. [12] used ALD to deposit a layer of amorphous Al_2O_3 on the surface of $\alpha-AlH_3$. The results showed that with the increase of coating cycles from 100 to 200, the decomposition temperature increased from $158.1\text{ }^\circ\text{C}$ to $161.2\text{ }^\circ\text{C}$ compared to $153.4\text{ }^\circ\text{C}$ for the uncoated sample. Figure 14 displays the SEM images of $\alpha-AlH_3@Al_2O_3$ particles after the hydrothermal aging test. It can be clearly seen that the surface of $\alpha-AlH_3$ particles after 200 coating cycles becomes much smoother than the uncoated one. Moreover, its friction sensitivity decreases from 96% to 68% after the hydrothermal aging test. The Al_2O_3 films can effectively impede the transfer of frictional heat to the AlH_3 core, thereby reducing the friction sensitivity of the core-shell structure.

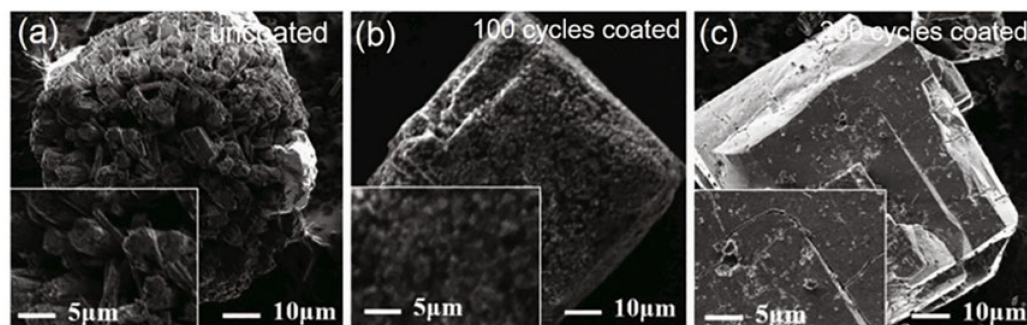


Figure 14. SEM images of α -AlH₃ stabilized by ALD method before and after. Hydrothermal aging test after ALD method (a) 0 cycles; (b,c) 100 and 200 cycles, respectively [12]. Copyright 2017, AVS.

4.3.3. Organic Polymers

Due to the non-energetic properties of small molecules as a coating layer for stabilization of AlH₃, the overall energy performance of the propellant will be attenuated. Therefore, the coating layer is preferably selected from the energetic components, such as nitrocellulose (NC). Flynn et al. [20] applied α -AlH₃ particles coated with nitrocellulose to a double-base solid propellant. As a result, the decomposition rate of AlH₃ was only 0.63% at 50 °C for 90 days, indicating that it had a significant stabilization effect.

Cai et al. [16] used supercritical fluid technology to cover the surface of α -AlH₃ with fluoroelastomer (FE26) uniformly. Total formation enthalpy (ΔH_f) of alane and alane/FE26 increased from -15.7 kJ/mol to -21.0 kJ/mol at heating rate of 20 °C, while Gibbs free energy (ΔG_f) decreased from 44 kJ/mol to 38.7 kJ/mol, indicating increased thermal stability. In electric spark sensitivity test, the E₅₀ value of alane is 63.71 mJ, and the value increased up to 85.24 mJ after 5% FE26 is coated on alane. This result indicates that after coating the FE26, safe electrostatic discharge can be achieved.

4.3.4. Carbon Materials

Su et al. [84] reported a novel method of coating AlH₃ with carbon nanotubes (CNT), where re-nucleation and growth of α -AlH₃ on the surface of the coating material, rather than the formation of the coating material on the surface of α -AlH₃ particles, occurred.

Xing et al. [15] attempted to improve the thermal stability of α -AlH₃ by using fullerene stabilizers (C₆₀), which allows α -AlH₃ to be stored at 60 °C for 3 months with a decomposition rate of less than 1%.

Li et al. [85] used the solvent-antisolvent method to coat α -AlH₃ with graphene oxide (GO). The α -AlH₃-GO material obtained was successfully applied to the solid propellant slurry, for which the mechanical impact sensitivity of slurry was effectively reduced, evidenced by an increase of the I₅₀ value from 7.3 J to 12.1 J.

4.3.5. Energetic Components

As mentioned above, increasing the content of this materials would undoubtedly reduce the energy density and detonation property of the propellants. Therefore, in order to achieve higher energy density, the coatings layer can be selected from stable energetic components.

Yu et al. [86] prepared the homogenous composites of AlH₃ and commonly used oxidizer (HMX, CL-20, and AP) using the in situ recrystallization method, for which thermal stability, compatibility, and ignition performance were investigated. The results showed that the initial decomposition temperatures of AlH₃/oxidizer are increased by about 16 °C, and the induction time of the dehydrogenation of AlH₃ is extended by 1.2 times. Such a stabilization effect of the oxidizers can be attributed to strong hydrogen bonding. Furthermore, the flame radiation intensity of each composite was enhanced, and the most intensive value of AlH₃/CL-20 is 3.4 times that of pure AlH₃. Moreover, the

crucible is even broken (marked with a white circle) when using AlH_3/AP composites as trigger for water-cooled CO_2 laser ignitor, as depicted in Figure 15.

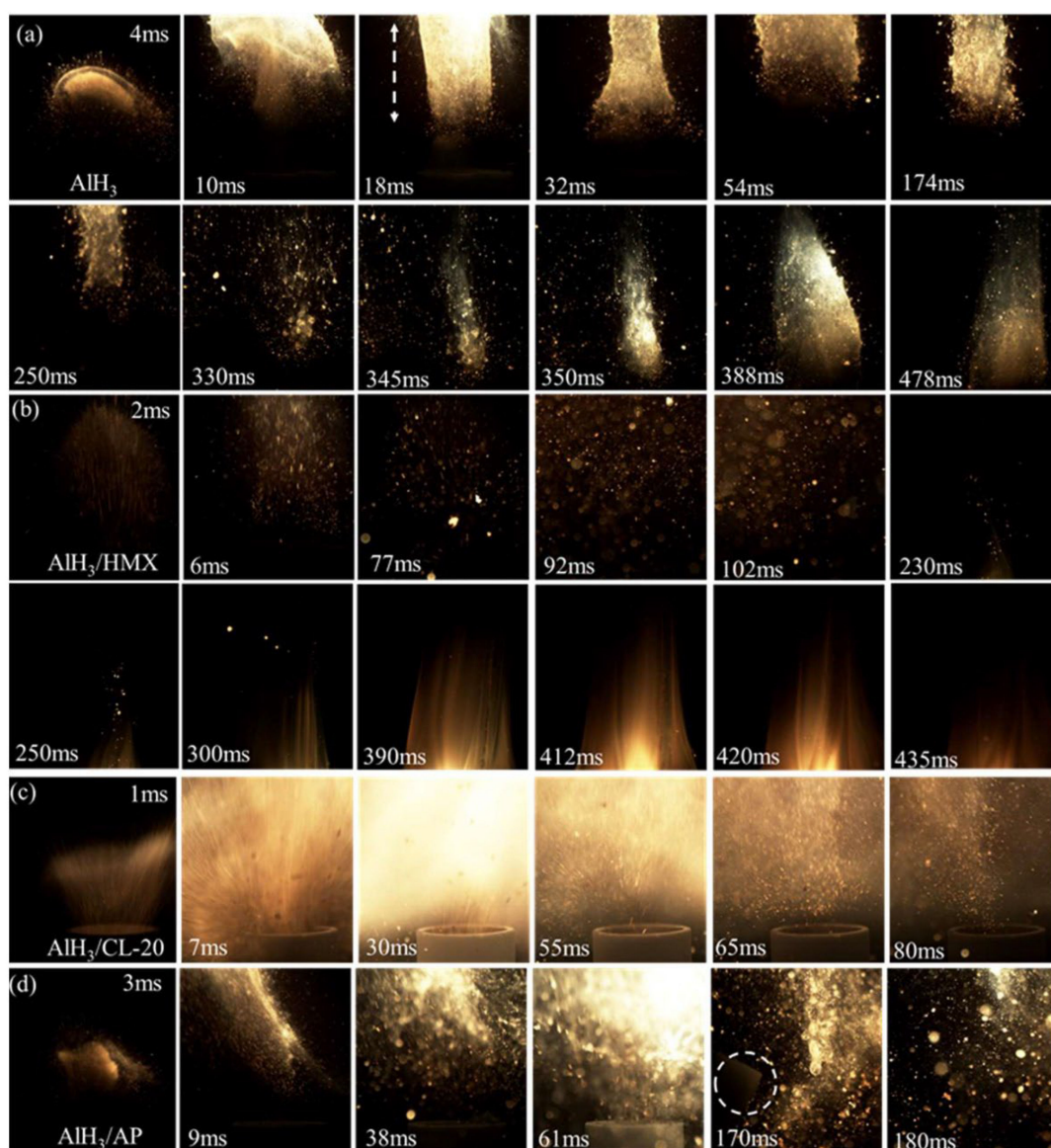


Figure 15. Flame images of raw AlH_3 and $\text{AlH}_3/\text{oxidizer}$ composites: (a) AlH_3 , (b) AlH_3/HMX , (c) $\text{AlH}_3/\text{CL-20}$, and (d) AlH_3/AP [86]. Copyright 2023, American Chemical Society.

Yu et al. [87] prepared fluoropolymer- and AP-coated AlH_3 -based composites (AHFPs) via a spray-drying technology aiming to improve the stability and combustion performance of AlH_3 . The results showed that the initial decomposition temperatures of AHFPs were increased by $17\text{ }^\circ\text{C}$, compared with pure AlH_3 . Moreover, the decomposition induction time was increased by 1.82 times compared to raw AlH_3 , indicating improved stability by the coatings of PFPE and AP. The maximum flame radiation intensity of AHFPs-30% is 7.71 times that of pure AlH_3 , suggests that the combustion performance of AlH_3 has also been enhanced. Table 4 summarizes the primary reported stabilization methods and properties of stabilized AlH_3 .

At present, the research of stabilizing of AlH_3 mainly focus on the surface coating method, involve the screening of the coating agent, especially energetic materials. However, how to accurately control the coating thickness so as to have better compatibility with the propellant components is the key for further research.

Table 4. The methods used for stabilizing and the resulting properties of AlH_3 .

Methods	Materials Used for Stabilization	$\alpha\text{-AlH}_3$ before Stabilization	$\alpha\text{-AlH}_3$ after Stabilization
Surface passivation	Mg and N-butylamine (H_2O) [15,70]	1% decomposition for 13.5 d at 60 °C	1% decomposition for 60 d at 60 °C
	$\text{C}_2\text{H}_5\text{OH}$ (98%) [70]	-	0.1% decomposition for 35–40 d at 60 °C
	Mg and $\text{KH}_2\text{PO}_4/\text{NaOH}$ [77]	-	0.25% decomposition for 49 d at 60 °C
	Mg, N-butylamine (H_2O) and $\text{KH}_2\text{PO}_4/\text{NaOH}$ [77]	1% decomposition for 33 d at 60 °C	1% decomposition for 43 d at 60 °C
	HCl solution [17]	1% decomposition for 9.3 d at 60 °C	1% decomposition for 12.7 d at 60 °C
	air (60 °C for 250 h) [72]	5% decomposition for 95 min at 115 °C	5% decomposition for 237 min at 115 °C
Doping	MBT/PTA [76]	7.5% decomposition for 14 d at 60 °C	PTA: 0.97% decomposition 60 °C for 27 d; MBT: 0.6% decomposition 60 °C for 17 d
	Hg [74]	9.4% decomposition for 24 h at 100 °C	0.4% decomposition for 24 h at 100 °C
	Mg [73]	1% decomposition for 5 d at 60 °C	1% decomposition for 26 d at 60 °C
	Si [74]	1% decomposition for 4 d at 60 °C	1% decomposition for 8 d at 60 °C
Surface coating	NO , N_2F_4 [80]	5.63% decomposition for 7 h at 100 °C	100 °C for 7 h, 0.21% decomposition
	Al_2S_3 [80]	Rapid decomposition for 2 h at 60 °C after store at room temperature for 114 d	0.13% decomposition for 22 h at 60 °C after store at room temperature for 114 d
	SA [18]	E_{50} : 367 mJ	E_{50} : 5390 mJ
	Diphenylacetylene [18]	1% decomposition for 13 d	0.84% decomposition for 48 d
	Nitrocellulose [20]	Rapid decomposition for 30 d at 50 °C, or for 10 d at 60 °C	0.3% decomposition for 90 d at 50 °C; 0.63% decomposition for 90 d at 60 °C
	FE26 [16]	E_{50} : 63.7 mJ	E_{50} : 85.24 mJ
	Al_2O_3 [12]	7.8% decomposition for 12 h at 70 °C	0.49% decomposition for 12 h at 70 °C
	GO [85]	I_{50} : 7.3 J	I_{50} : 12.1 J
C_{60} [15]	-	<1% decomposition for 90 d at 60 °C	

Note: MBT: 2-Mercaptobenzothiazole; PTA: Phenothiazine; E_{50} : electrostatic spark sensitivity; I_{50} : impact sensitivity; SA: Stearic acid.

5. High Energy Fuel for Solid Propellant

Compared with aluminum powder, a wildly metal fuel adopted to improve the energy characteristics of composite propellants [88,89], AlH_3 has extraordinary potential in the application of solid propellant. NASA CEA results indicate that replacing aluminum with AlH_3 will increase specific impulse by 10% [90] over AP/HTPB rocket propellant and reduce flame temperature by 5% [91]. Furthermore, AlH_3 produces more H_2 and H_2O in the combustion products, reducing the mole fraction of combustion product. Shark et al., found the use of AlH_3 hydride additives could raise the overall specific impulse of DCPD/RGHP by 4% [92]. Maggi et al., demonstrated a 6–8% gain in gravimetric specific impulse gain for the aluminum and lithium aluminum hydrides when aluminized AP/HTPB compositions were chosen as a Reference [91].

The ballistic and physical properties of propellants based on AlH_3 were investigated experimentally [3]. As depicted in Figure 16a–c, the flame intensity of AlH_3 -based propellants is significantly lower compared to micron and nano-aluminized solid propellants, indicating a lower adiabatic temperature. Another difference lies in the aggregation/agglomeration processes on the burning surface. Figure 15d illustrates that the high burning rate of AlH_3 -based propellants can effectively prevent the aggregation phenomenon.

Bazyn et al. [93] studied the combustion characteristics of AlH_3 under the condition of a solid rocket motor. The experimental results show that the decomposition time of AlH_3 is exponentially correlated with temperature, which satisfies the Arrhenius type rate equation.

Although AlH_3 has been used as energy fuel for solid propellant. The intrinsic metastability affects its further practical application. The easy decomposition of AlH_3 causes concern for the safe storage and continuous combustion of the propellant system.

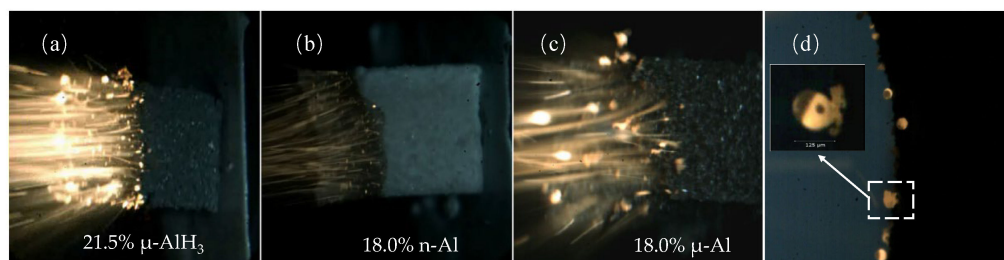


Figure 16. (a–c) The flame structures observed during the combustion of AlH₃-based propellants; (d) the burning surface [3]. Copyright 2007, Elsevier.

6. Conclusions and Suggestions

AlH₃ is a binary metal hydride with seven known polymorphs among which α is the most stable. Due to the high volumetric energy density of AlH₃, the introduction into solid propellant is helpful to provide a large amount of energy via combustion. In this paper, the synthesis methods, key properties, and tuning of AlH₃ are presented, with the following conclusions drawn:

1. The commonly used methods of synthesizing AlH₃ are wet chemical synthesis and mechano-chemical method, both of which are faced with the difficulty in achieving high crystal purity of the product. Adding crystalline inducer helps to control the proportion of crystal types, but the presence of an inducer in the product will lead to a decrease in the thermal stability of AlH₃. Therefore, highly effective inducers are easy to separate, and need to be developed.
2. From a kinetics perspective, the acceleratory period is a critical stage that governs the decomposition rate of aluminum hydride, primarily due to the multi-dimensional growth of the aluminum phase. However, the acceleration period is difficult to control. Thus, how to decelerate the decomposition rate by prolonging the induction period through modifying the surface components of AlH₃ is the next research direction.
3. The stabilization of AlH₃ involves enhancing crystal purity, isolating from external stimuli, and eliminating factors contributing to instability. Among the stabilization methods, surface passivation and the doping method will cause energy loss and negatively affect the combustion performance. As for surface coating, the ratio and thickness of the coating layer proves difficult to control, resulting in failure to accurately regulate its impact on the energy performance of α -AlH₃. Efficient coating materials are crucial for advancing the application of AlH₃ in solid propellants.

Author Contributions: Writing—original draft preparation, Y.L.; writing—review and editing, F.Y.; investigation and supervision, Z.W. and Z.Z.; data curation and funding acquisition, Y.Z. All authors have read and agreed to the published version of the manuscript.

Funding: This research received no external funding.

Data Availability Statement: No new data were created or analyzed in this study. Data sharing is not applicable to this article.

Conflicts of Interest: Author Yang Zhang was employed by the company Xi'an Modern Chemistry Research Institute. The remaining authors declare that the research was conducted in the absence of any commercial or financial relationships that could be construed as a potential conflict of interest.

References

1. Young, G.; Risha, G.A.; Connell, T.L.; Yetter, R.A. Combustion of HTPB Based Solid Fuels Containing Metals and Metal Hydrides with Nitrous Oxide. *Propellants Explos. Pyrotech.* **2019**, *44*, 744–750. [[CrossRef](#)]
2. Chen, S.; Tang, Y.; Yu, H.; Bao, L.; Zhang, W.; DeLuca, L.T.; Shen, R.; Ye, Y. The Rapid H₂ Release from AlH₃ Dehydrogenation Forming Porous Layer in AlH₃/Hydroxyl-Terminated Polybutadiene (HTPB) Fuels during Combustion. *J. Hazard. Mater.* **2019**, *371*, 53–61. [[CrossRef](#)]

3. DeLuca, L.T.; Galfetti, L.; Severini, F.; Rossettini, L.; Meda, L.; Marra, G.; D'Andrea, B.; Weiser, V.; Calabro, M.; Vorozhtsov, A.B.; et al. Physical and Ballistic Characterization of AlH₃-Based Space Propellants. *Aerosp. Sci. Technol.* **2007**, *11*, 18–25. [[CrossRef](#)]
4. Ding, X.; Shu, Y.; Liu, N.; Wu, M.; Zhang, J.; Gou, B.; Wang, H.; Wang, C.; Dong, S.; Wang, W. Energetic Characteristics of HMX-Based Explosives Containing LiH. *Propellants Explos. Pyrotech.* **2016**, *41*, 1079–1084. [[CrossRef](#)]
5. Liu, L.; Li, J.; Zhang, L.; Tian, S. Effects of Magnesium-Based Hydrogen Storage Materials on the Thermal Decomposition, Burning Rate, and Explosive Heat of Ammonium Perchlorate-Based Composite Solid Propellant. *J. Hazard. Mater.* **2018**, *342*, 477–481. [[CrossRef](#)]
6. Yang, Z.; Zhao, F.; Xu, S.; Yang, F.; Yao, E.; Ren, X.; Wu, Z.; Zhang, Z. Investigation on Adsorption and Decomposition Properties of CL-20/FOX-7 Molecules on MgH₂(110) Surface by First-Principles. *Molecules* **2020**, *25*, 2726. [[CrossRef](#)]
7. Pang, W.; Fan, X.; Zhao, F.; Xu, H.; Zhang, W.; Yu, H.; Li, Y.; Liu, F.; Xie, W.; Yan, N. Effects of Different Metal Fuels on the Characteristics for HTPB-based Fuel Rich Solid Propellants. *Propellants Explos. Pyrotech.* **2013**, *38*, 852–859. [[CrossRef](#)]
8. Cooper, M.A.; Oliver, M.S. The Burning Regimes and Conductive Burn Rates of Titanium Subhydride Potassium Perchlorate (TiH_{1.65}/KClO₄) in Hybrid Closed Bomb-Strand Burner Experiments. *Combust. Flame* **2013**, *160*, 2619–2630. [[CrossRef](#)]
9. Bi, X.; Liu, J. Detonation Properties of High Explosives Containing Ammonia Borane. *Z. Anorg. Allg. Chem.* **2016**, *642*, 773–777. [[CrossRef](#)]
10. Li, H.; Liang, D.; Yu, M.; Liu, J.; Wang, Y.; Pang, A.; Tang, G.; Huang, X. Study on Dehydrogenation and Oxidation Kinetics Mechanisms of Micron α -AlH₃ in an Oxidative Atmosphere. *Int. J. Hydrogen Energy* **2020**, *45*, 24958–24967. [[CrossRef](#)]
11. Graetz, J.; Reilly, J.J.; Yartys, V.A.; Maehlen, J.P.; Bulychev, B.M.; Antonov, V.E.; Tarasov, B.P.; Gabis, I.E. Aluminum Hydride as a Hydrogen and Energy Storage Material: Past, Present and Future. *J. Alloys Compd.* **2011**, *509*, S517–S528. [[CrossRef](#)]
12. Chen, R.; Duan, C.L.; Liu, X.; Qu, K.; Tang, G.; Xu, X.-X.; Shan, B. Surface Passivation of Aluminum Hydride Particles via Atomic Layer Deposition. *J. Vac. Sci. Technol. A Vac. Surf. Film.* **2017**, *35*, 03E111. [[CrossRef](#)]
13. Jiang, Z.F.; Zhao, F.Q.; Zhang, M.; Li, H.; Zhang, J.-K.; Yang, Y.-J.; Li, N. Research Progress in the Stabilization of Aluminum Hydride. *Huozhayao Xuebao/Chin. J. Explos. Propellants* **2020**, *43*, 107–115. [[CrossRef](#)]
14. Qin, M.-N.; Zhang, Y.; Tang, W.; Shi, Q.; Wang, W.; Qiu, S.-J. α -AlH₃ Coated with Stearic Acid: Preparation and Its Electrostatic Sensitivity. *Hanneng Cailiao/Chin. J. Energ. Mater.* **2017**, *25*, 59–62. [[CrossRef](#)]
15. Xing, J.H.; Xia, Y.; Wang, J.W. A Method for Improving Thermal Stability of Aluminum Hydride. CN Patent 109019507A, 5 November 2021. pp. 11–15.
16. Cai, X.W.; Yang, J.H.; Zhang, J.L.; Ma, D.X.; Wang, Y.P. Liquid Carbon Dioxide as Anti-Solvent Coating Aluminum Hydride. *Propellants Explos. Pyrotech.* **2016**, *40*, 914–919. [[CrossRef](#)]
17. Petrie, M.A.; Bottaro, J.C.; Schmitt, R.J.; Penwell, P.E.; Bomberger, D.C. Preparation of Aluminum Hydride Polymorphs, Particularly Stabilized α -AlH₃. U.S. Patent 6228338, 8 May 2001. pp. 5–8.
18. Schmidt, D. Non-Solvated Particulate Aluminum Hydride Coated with a Cyano-Coating Compound Useful in Solid Propellants. U.S. Patent 3850709, 26 November 1974. pp. 11–26.
19. Roberts, C.B.; Toner, D.D. Stabilization of Light Metal Hydride (U). U.S. Patent 3850709, 26 November 1974. pp. 11–26.
20. Flynn, J. Particulate Aluminum Hydride with Nitrocellulose Coating Suitable for Use in Solid Propellants. U.S. Patent 3855022, 17 December 1974. pp. 12–17.
21. Finholt, A.E.; Bond, A.C.; Schlesinger, H.I. Lithium Aluminum Hydride, Aluminum Hydride and Lithium Gallium Hydride, and Some of Their Applications in Organic and Inorganic Chemistry 1. *J. Am. Chem. Soc.* **1947**, *69*, 1199–1203. [[CrossRef](#)]
22. Brower, F.M.; Matzek, N.E.; Reigler, P.F.; Rinn, H.W.; Roberts, C.B.; Schmidt, D.L.; Snover, J.A.; Terada, K. Preparation and Properties of Aluminum Hydride. *J. Am. Chem. Soc.* **1976**, *98*, 2450–2453. [[CrossRef](#)]
23. Yu, M.; Zhu, Z.; Li, H.-P.; Yan, Q.-L. Advanced Preparation and Processing Techniques for High Energy Fuel AlH₃. *Chem. Eng. J.* **2021**, *421*, 129753. [[CrossRef](#)]
24. Park, M.; Kim, W.; Kwon, Y.; Kim, J.; Jo, Y. Wet Synthesis of Energetic Aluminum Hydride. *Propellants Explos. Pyrotech.* **2019**, *44*, 1233–1241. [[CrossRef](#)]
25. Xu, B.; Liu, J.; Wang, X. Preparation and Thermal Properties of Aluminum Hydride Polymorphs. *Vacuum* **2014**, *99*, 127–134. [[CrossRef](#)]
26. Xu, B.; Liu, J.P. Aluminum Hydride Polymorphs: Preparation, Characterization and Thermal Properties. *Adv. Mater. Res.* **2013**, *712–715*, 333–336. [[CrossRef](#)]
27. Liu, H.; Zhang, L.; Ma, H.; Lu, C.; Luo, H.; Wang, X.; Huang, X.; Lan, Z.; Guo, J. Aluminum Hydride for Solid-State Hydrogen Storage: Structure, Synthesis, Thermodynamics, Kinetics, and Regeneration. *J. Energy Chem.* **2021**, *52*, 428–440. [[CrossRef](#)]
28. Paskevicius, M.; Sheppard, D.A.; Buckley, C.E. Characterisation of Mechanochemically Synthesised Alane (AlH₃) Nanoparticles. *J. Alloys Compd.* **2009**, *487*, 370–376. [[CrossRef](#)]
29. Duan, C.W.; Hu, L.X.; Xue, D. Solid State Synthesis of Nano-Sized AlH₃ and Its Dehydriding Behaviour. *Green Chem.* **2015**, *17*, 3466–3474. [[CrossRef](#)]
30. Duan, C.; Cao, Y.; Hu, L.; Fu, D.; Ma, J.; Youngblood, J. An Efficient Mechanochemical Synthesis of Alpha-Aluminum Hydride: Synergistic Effect of TiF₃ on the Crystallization Rate and Selective Formation of Alpha-Aluminum Hydride Polymorph. *J. Hazard. Mater.* **2019**, *373*, 141–151. [[CrossRef](#)] [[PubMed](#)]
31. Kim, Y.; Lee, E.-K.; Shim, J.-H.; Cho, Y.W.; Yoon, K.B. Mechanochemical Synthesis and Thermal Decomposition of Mg(AlH₄)₂. *J. Alloys Compd.* **2006**, *422*, 283–287. [[CrossRef](#)]

32. Baranowski, B.; Tkacz, M. The Equilibrium Between Solid Aluminium Hydride and Gaseous Hydrogen. *Z. Phys. Chem.* **1983**, *135*, 27–38. [[CrossRef](#)]
33. Appel, M.; Frankel, J.P. Production of Aluminum Hydride by Hydrogen-Ion Bombardment. *J. Chem. Phys.* **1965**, *42*, 3984–3988. [[CrossRef](#)]
34. Saitoh, H.; Machida, A.; Katayama, Y.; Aoki, K. Formation and Decomposition of AlH₃ in the Aluminum-Hydrogen System. *Appl. Phys. Lett.* **2008**, *93*, 151918. [[CrossRef](#)]
35. Dymova, T.N.; Mal'tseva, N.N.; Konoplev, V.N.; Golovanova, A.I.; Aleksandrov, D.P.; Sizareva, A.S. Solid-Phase Solvate-Free Formation of Magnesium Hydroaluminates Mg(AlH₄)₂ and MgAlH₅ upon Mechanochemical Activation or Heating of Magnesium Hydride and Aluminum Chloride Mixtures. *Russ. J. Coord. Chem. Khim.* **2003**, *29*, 385–389. [[CrossRef](#)]
36. Dymova, T.N.; Konoplev, V.N.; Sizareva, A.S.; Aleksandrov, D.P. Magnesium Tetrahydroaluminate: Solid-Phase Formation with Mechanochemical Activation of a Mixture of Aluminum and Magnesium Hydrides. *Russ. J. Coord. Chem. Khim.* **1999**, *25*, 312–315.
37. Fichtner, M.; Frommen, C.; Fuhr, O. Synthesis and Properties of Calcium Alanate and Two Solvent Adducts. *Inorg. Chem.* **2005**, *44*, 3479–3484. [[CrossRef](#)] [[PubMed](#)]
38. Mal'tseva, N.N.; Golovanova, A.I.; Dymova, T.N.; Aleksandrov, D.P. Solid-Phase Formation of Calcium Hydridoaluminates Ca(AlH₄)₂ and CaHAlH₄ upon Mechanochemical Activation or Heating of Mixtures of Calcium Hydride with Aluminum Chloride. *Russ. J. Inorg. Chem.* **2001**, *46*, 1793–1797.
39. Mamatha, M.; Bogdanović, B.; Felderhoff, M.; Pommerin, A.; Schmidt, W.; Schüth, F.; Weidenthaler, C. Mechanochemical Preparation and Investigation of Properties of Magnesium, Calcium and Lithium–Magnesium Alanates. *J. Alloys Compd.* **2006**, *407*, 78–86. [[CrossRef](#)]
40. Duan, C.; Hu, L.; Sun, Y.; Zhou, H.; Yu, H. An Insight into the Process and Mechanism of a Mechanically Activated Reaction for Synthesizing AlH₃ Nano-Composites. *Dalt. Trans.* **2015**, *44*, 16251–16255. [[CrossRef](#)] [[PubMed](#)]
41. Duan, C.; Cao, Y.; Hu, L.; Fu, D.; Ma, J. Synergistic Effect of TiF₃ on the Dehydrogenating Property of α -AlH₃ Nano-Composite. *Mater. Lett.* **2019**, *238*, 254–257. [[CrossRef](#)]
42. Wang, L.; Rawal, A.; Quadir, M.Z.; Aguey-Zinsou, K.-F. Formation of Aluminium Hydride (AlH₃) via the Decomposition of Organoaluminium and Hydrogen Storage Properties. *Int. J. Hydrogen Energy* **2018**, *43*, 16749–16757. [[CrossRef](#)]
43. Liu, H.; Bouchard, M.; Zhang, L. An Experimental Study of Hydrogen Solubility in Liquid Aluminium. *J. Mater. Sci.* **1995**, *30*, 4309–4315. [[CrossRef](#)]
44. Mcgrady, G.S. Hydrogenation of Aluminum Using a Supercritical Fluid Medium. U.S. Patent 0241056, 6 December 2008. pp. 10–12.
45. Liu, F.; Huang, K.; Wu, Q.; Dai, S. Solvent-Free Self-Assembly to the Synthesis of Nitrogen-Doped Ordered Mesoporous Polymers for Highly Selective Capture and Conversion of CO₂. *Adv. Mater.* **2017**, *29*, 1700445. [[CrossRef](#)]
46. Zidan, R.; Garcia-Diaz, B.L.; Fewox, C.S.; Stowe, A.C.; Gray, J.R.; Harter, A.G. Aluminium Hydride: A Reversible Material for Hydrogen Storage. *Chem. Commun.* **2009**, *35*, 3717. [[CrossRef](#)]
47. Saitoh, H.; Okajima, Y.; Yoneda, Y.; Machida, A.; Kawana, D.; Watanuki, T.; Katayama, Y.; Aoki, K. Formation and Crystal Growth Process of AlH₃ in Al–H System. *J. Alloys Compd.* **2010**, *496*, L25–L28. [[CrossRef](#)]
48. Sinke, G.C.; Walker, L.C.; Oetting, F.L.; Stull, D.R. Thermodynamic Properties of Aluminum Hydride. *J. Chem. Phys.* **1967**, *47*, 2759–2761. [[CrossRef](#)]
49. Chizinsky, G.; Evans, G.G.; Gibb, T.R.P.; Rice, M.J. Non-Solvated Aluminum Hydride 1. *J. Am. Chem. Soc.* **1955**, *77*, 3164–3165. [[CrossRef](#)]
50. Sartori, S.; Opalka, S.M.; Løvvik, O.M.; Guzik, M.N.; Tang, X.; Hauback, B.C. Experimental Studies of α -AlD₃ and α' -AlD₃ versus First-Principles Modelling of the Alane Isomorphs. *J. Mater. Chem.* **2008**, *18*, 2361. [[CrossRef](#)]
51. Graetz, J.; Reilly, J.J.; Kulleck, J.G.; Bowman, R.C. Kinetics and Thermodynamics of the Aluminum Hydride Polymorphs. *J. Alloys Compd.* **2007**, *446–447*, 271–275. [[CrossRef](#)]
52. Maehlen, J.P.; Yartys, V.A.; Denys, R.V.; Fichtner, M.; Frommen, C.; Bulychev, B.M.; Pattison, P.; Emerich, H.; Filinchuk, Y.E.; Chernyshov, D. Thermal Decomposition of AlH₃ Studied by in Situ Synchrotron X-Ray Diffraction and Thermal Desorption Spectroscopy. *J. Alloys Compd.* **2007**, *446–447*, 280–289. [[CrossRef](#)]
53. Liu, H.; Wang, X.; Dong, Z.; Cao, G.; Liu, Y.; Chen, L.; Yan, M. Dehydrogenating Properties of γ -AlH₃. *Int. J. Hydrogen Energy* **2013**, *38*, 10851–10856. [[CrossRef](#)]
54. Gao, S.; Liu, H.; Wang, X.; Xu, L.; Liu, S.; Sheng, P.; Zhao, G.; Wang, B.; Li, H.; Yan, M. Hydrogen Desorption Behaviors of γ -AlH₃: Diverse Decomposition Mechanisms for the Outer Layer and the Inner Part of γ -AlH₃ Particle. *Int. J. Hydrogen Energy* **2017**, *42*, 25310–25315. [[CrossRef](#)]
55. Graetz, J.; Reilly, J.J. Thermodynamics of the α , β and γ Polymorphs of AlH₃. *J. Alloys Compd.* **2006**, *424*, 262–265. [[CrossRef](#)]
56. Stavila, V.; Li, S.; Dun, C.; Marple, M.A.T.; Mason, H.E.; Snider, J.L.; Reynolds, J.E.; El Gabaly, F.; Sugar, J.D.; Spataru, C.D.; et al. Defying Thermodynamics: Stabilization of Alane Within Covalent Triazine Frameworks for Reversible Hydrogen Storage. *Angew. Chem.* **2021**, *133*, 26019–26028. [[CrossRef](#)]
57. Herley, P.J.; Christofferson, O.; Irwin, R. Decomposition of Alpha-Aluminum Hydride Powder. 1. Thermal Decomposition. *J. Phys. Chem.* **1981**, *85*, 1874–1881. [[CrossRef](#)]
58. Herley, P.J.; Christofferson, O. Decomposition of Alpha-Aluminum Hydride Powder. 2. Photolytic Decomposition. *J. Phys. Chem.* **1981**, *85*, 1882–1886. [[CrossRef](#)]

59. Herley, P.J.; Christofferson, O. Decomposition of Alpha.-Aluminum Hydride Powder. 3. Simultaneous Photolytic-Thermal Decomposition. *J. Phys. Chem.* **1981**, *85*, 1887–1892. [[CrossRef](#)]
60. Tarasov, V.P.; Muravlev, Y.B.; Bakum, S.I.; Novikov, A.V. Kinetics of Formation of Metallic Aluminum upon Thermal and Photolytic Decomposition of Aluminum Trihydride and Trideuteride as Probed by NMR. *Dokl. Phys. Chem.* **2003**, *393*, 353–356. [[CrossRef](#)]
61. Milekhin, Y.M.; Koptelov, A.A.; Matveev, A.A.; Baranets, Y.N.; Bakulin, D.A. Studying Aluminum Hydride by Means of Thermal Analysis. *Russ. J. Phys. Chem. A* **2015**, *89*, 1141–1145. [[CrossRef](#)]
62. Kato, S.; Biemann, M.; Ikeda, K.; Orimo, S.; Borgschulte, A.; Züttel, A. Surface Changes on AlH₃ during the Hydrogen Desorption. *Appl. Phys. Lett.* **2010**, *96*, 051912. [[CrossRef](#)]
63. Liu, J.; Yuan, J.; Li, H.; Pang, A.; Xu, P.; Tang, G.; Xu, X. Thermal Oxidation and Heterogeneous Combustion of AlH₃ and Al: A Comparative Study. *Acta Astronaut.* **2021**, *179*, 636–645. [[CrossRef](#)]
64. Duan, C.W.; Hu, L.X.; Sun, Y.; Zhou, H.P.; Yu, H. Reaction Kinetics for the Solid State Synthesis of the AlH₃/MgCl₂ Nano-Composite by Mechanical Milling. *Phys. Chem. Chem. Phys.* **2015**, *17*, 22152–22159. [[CrossRef](#)]
65. Nakagawa, Y.; Isobe, S.; Wang, Y.; Hashimoto, N.; Ohnuki, S.; Zeng, L.; Liu, S.; Ichikawa, T.; Kojima, Y. Dehydrogenation Process of AlH₃ Observed by TEM. *J. Alloys Compd.* **2013**, *580*, S163–S166. [[CrossRef](#)]
66. Yu, M.H.; Xie, W.X.; Zhu, Z.Y.; Yan, Q.L. Stability, Reactivity and Decomposition Kinetics of Surface Passivated α -AlH₃ Crystals. *Int. J. Hydrogen Energy* **2022**, *47*, 8916–8928. [[CrossRef](#)]
67. Evard, E.A.; Voyt, A.P. Hydride Decomposition Characterization by Means of “Morphological Trajectory” Method—Applied to AlH₃. *J. Alloys Compd.* **2011**, *509*, S667–S670. [[CrossRef](#)]
68. Gabis, I.E.; Voyt, A.P.; Chernov, I.A.; Kuznetsov, V.G.; Baraban, A.P.; Elets, D.I.; Dobrotvorsky, M.A. Ultraviolet Activation of Thermal Decomposition of α -Alane. *Int. J. Hydrogen Energy* **2012**, *37*, 14405–14412. [[CrossRef](#)]
69. Pang, A.; Zhu, Z.; Xu, X. Recent Progresses on Synthesis and Evaluation of AlH₃. *Chin. J. Energ. Mater.* **2019**, *27*, 317–325.
70. Niles, E.T.; Seaman, B.A.; Wilson, E.J. Stabilization of Aluminum Hydride. U.S. Patent 3869544, 28 June 1975. pp. 3–4.
71. Roberts, C.B. Stabilization of Aluminum Hydride. U.S. Patent 3821044, 28 June 1974.
72. Nylack, G.A. Method for Increasing the Thermal Stability of Aluminum Hydride Storage. RU Patent 2175637, 8 May 2001. pp. 5–8.
73. Norman, M.E.; Herbert, R.C. Stabilization of Light Metal Hydride. U.S. Patent 3857922, 9 April 1974. pp. 12–31.
74. Cianciolo, A.; Sabatine, S.J. Process for the Preparation of Mercury-Coating Aluminum Hydride Compositions. U.S. Patent 3785890, 15 January 1974. pp. 1–15.
75. Xing, X.H.; Xia, Y.; Zhang, X.Q.; Chang, W.L.; Wang, J.W. Research Progress in Improving Thermal Stability of Aluminum Trihydride. *Chem. Propellants Polym. Mater.* **2018**, *16*, 21–25.
76. Ardis, A.; Natoli, F. Thermal Stability of Aluminum Hydride through Use of Stabilizers. U.S. Patent 3801707, 2 April 1974. pp. 4–12.
77. Roberts, C.B.; Toner, D.D. Stabilization of Light Metalhydride(U). U.S. Patent 3803082, 9 April 1974. pp. 4–9.
78. Maycock, J.N.; Paiverneker, V.R. *Crystal Lattice Doping Studies of High Energy Propellant Ingredients AD-507040*; Defense Technical Information Center: Fort Belvoir, VA, USA, 1969.
79. Wang, K.; Liu, Z.; Wang, X.; Cui, X. Enhancement of Hydrogen Binding Affinity with Low Ionization Energy Li₂F Coating on C60 to Improve Hydrogen Storage Capacity. *Int. J. Hydrogen Energy* **2014**, *39*, 15639–15645. [[CrossRef](#)]
80. Norman, M.E. Non-Solvated Aluminum Hydride Coated with Stabilizer. U.S. Patent 3844853, 29 October 1974.
81. Shi, Z.; Lu, T.; Zhang, J.; Zhu, Z.; Xu, Y.; Xia, D.; Hu, Y.; Lin, K.; Yang, Y. The Enhanced Thermal Stability and Reduced Hygroscopicity of Aluminum Hydride Coated with Vinyltrimethoxysilane. *New J. Chem.* **2022**, *46*, 1643–1649. [[CrossRef](#)]
82. Kempa, P.B.; Thome, V.; Herrmann, M. Structure, Chemical and Physical Behavior of Aluminum Hydride. *Part. Part. Syst. Charact.* **2009**, *26*, 132–137. [[CrossRef](#)]
83. Qin, J.; Gong, T.; Yan, N.; Li, J.G.; Hui, L.F.; Hao, H.X. Research Progress on Application of Atomic Layer Deposition in Surface Fabrication of Energetic Material. *Chin. J. Explos. Propellant* **2019**, *42*, 425–431.
84. Su, J.; Li, J.; Guan, H.B. A Method for Coating Aluminum Hydride with Carbon Nanotubes. CN 108163839A, 15 June 2018.
85. Li, L. Desensitization of Aluminum Hydride (AlH₃) by Graphene Oxide. *Chin. J. Solid Rocket Technol.* **2019**, *42*, 66–71.
86. Yu, M.H.; Yang, S.L.; Xie, W.X.; Zhu, Z.Y.; Li, H.P.; Yan, Q.L. Enhanced Stability and Combustion Performance of AlH₃ in Combination with Commonly Used Oxidizers. *Fuel* **2023**, *331*, 125741. [[CrossRef](#)]
87. Yu, M.H.; Yang, S.L.; Xie, W.X.; Li, Y.J.; Li, H.P.; Yan, Q.L. Stabilization of AlH₃ Crystals by the Coating of Hydrophobic PFPE and Resulted Reactivity with Ammonium Perchlorate. *Langmuir* **2023**, *39*, 7863–7875. [[CrossRef](#)] [[PubMed](#)]
88. Pang, W.; Luigi, D.T.; Fan, X.; Wang, K.; Li, J.; Zhao, F. Progress on Modification of High Active Aluminum Powder and Combustion Agglomeration in Chemical Propellants. *J. Solid Rocket Technol.* **2019**, *42*, 42–53.
89. Cheng, Z.P.; He, X.X. Research Progress of Nano Aluminum Fuel. *J. Solid Rocket Technol.* **2017**, *40*, 437–447.
90. Bazyn, T.; Eyer, R.; Krier, H.; Glumac, N. Combustion Characteristics of Aluminum Hydride at Elevated Pressure and Temperature. *J. Propuls. Power* **2004**, *20*, 427–431. [[CrossRef](#)]
91. Maggi, F.; Gariani, G.; Galfetti, L.; DeLuca, L.T. Theoretical Analysis of Hydrides in Solid and Hybrid Rocket Propulsion. *Int. J. Hydrogen Energy* **2012**, *37*, 1760–1769. [[CrossRef](#)]

92. Shark, S.; Sippel, T.; Son, S.; Heister, S.; Pourpoint, T. Theoretical Performance Analysis of Metal Hydride Fuel Additives for Rocket Propellant Applications. In Proceedings of the 47th AIAA/ASME/SAE/ASEE Joint Propulsion Conference & Exhibit, San Diego, CA, USA, 31 July–3 August 2011.
93. Bazyn, T.; Krier, H.; Glumac, N.; Shankar, N.; Wang, X.; Jackson, T.L. Decomposition of Aluminum Hydride Under Solid Rocket Motor Conditions. *J. Propuls. Power* **2007**, *23*, 457–464. [[CrossRef](#)]

Disclaimer/Publisher’s Note: The statements, opinions and data contained in all publications are solely those of the individual author(s) and contributor(s) and not of MDPI and/or the editor(s). MDPI and/or the editor(s) disclaim responsibility for any injury to people or property resulting from any ideas, methods, instructions or products referred to in the content.